Cell Reports, Volume *25*

Supplemental Information

Importin α5 Regulates Anxiety through MeCP2 and Sphingosine Kinase 1

Nicolas Panayotis, Anton Sheinin, Shachar Y. Dagan, Michael M. Tsoory, Franziska Rother, Mayur Vadhvani, Anna Meshcheriakova, Sandip Koley, Letizia Marvaldi, Didi-Andreas Song, Eitan Reuveny, Britta J. Eickholt, Enno Hartmann, Michael Bader, Izhak Michaelevski, and Mike Fainzilber

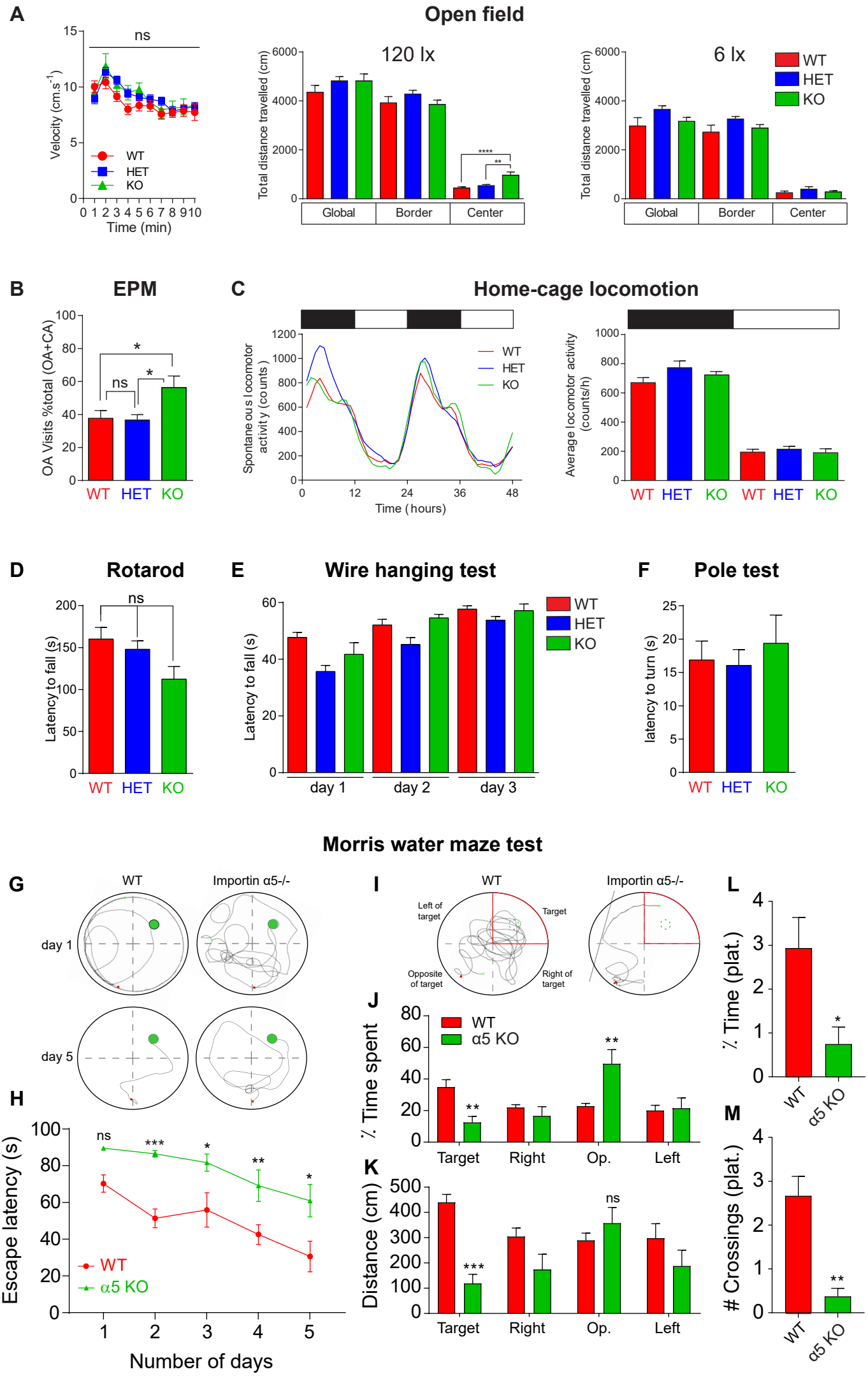
A
Open field
ns
Velocity (cm.s-1)
Time (min)
WT
HET
KO
120 lx
6 lx
Total distance travelled (cm)
Global
Border
Center
B
EPM
OA Visits %total (OA+CA)
C
Home-cage locomotion
Spontaneous locomotor activity (counts)
Time (hours)
Average locomotor activity (counts/h)
D
Rotarod
Latency to fall (s)
E
Wire hanging test
day 1
day 2
day 3
F
Pole test
latency to turn (s)
Morris water maze test
G
WT
Importin α5-/-
day 1
day 5
H
Escape latency (s)
Number of days
α5 KO
I
Left of target
Target
Opposite of target
Right of target
J
% Time spent
Target
Right
Op.
Left
K
Distance (cm)
L
% Time (plat.)
M
Crossings (plat.)

Fig. S1 (*Related to Fig. 2*)**. Preserved sensory and motor performance and impaired Morris water maze performances in importin α5 knockout mice. A**, importin α5 KO movement speed (green) was not significantly different over the 10 min of the OF session compared to WT (red) and HET (blue) littermates. Reducing OF illumination from 120 to 6 lux abolished differences between WT and importin α5 KO animals in the distance travelled in the OF center area. **B**, importin α5 KO mice show increased exploration of EPM open arms (expressed as a percentage of open arm visits from the total number of visits to all arms) ($p < 0.05$). **C**, Circadian activity over 48 hrs shows that the home-cage activity of importin α5 KO was not different from WT and HET during the dark and light phases (black and white boxes above the graphs, respectively). **D**, accelerated rotarod, **E**, wire hanging test and **F**, pole test, all confirm the absence of locomotion and coordination/balance defects in importin α5 KO animals. $n \geq 6$ animals for each genotype per test. **G-H**, Importin α5 knockout mice showed altered performance during the spatial acquisition phase of the Morris water maze. Mice were subjected to 4 trials per day with an interval of 10 min, for 5 consecutive days (See Methods). G, Representative swimming paths for each genotype at day 1 and day 5 (end of acquisition). The green circle depicts the location of the hidden platform and the dashed lines demarcates the 4 quadrants. H, Escape latency (in seconds) over time during training sessions in the Morris water maze. **I-M**, Importin α5 knockout do not actively search for the escape platform. **I**, Representative swimming paths for the probe test session (24hrs after acquisition – dashed green circles mark where the hidden platform was located during training and the target quadrant appears in red). **J**, The percentage time spent in each of the quadrants during the probe test (target, right of target, opposite of target, left of target) shows that importin α5 knockout spent less time scanning the target quadrant while they spent more time in the opposite one compared to their wild-type littermates. **K**, The distance covered during the probe test suggests that importin α5 knockouts explore the target quadrant less, but do not compensate by swimming more in the other quadrants during the session. **L**, Percentage time spent and **M**, Number of crossing over the platform location. n=9 WT; n=8 Importin α5 KO. * $p < 0.05$; ** $p < 0.01$, *** $p < 0.001$ (one-way ANOVA followed by Tukey's HSD post hoc correction for multiple comparisons (**A-F**); Two-way ANOVA followed by Sidak post-hoc analysis test (**H, J, K**) and Mann-Whitney test (**L, M**)). All data error bars represent mean +/- SEM.

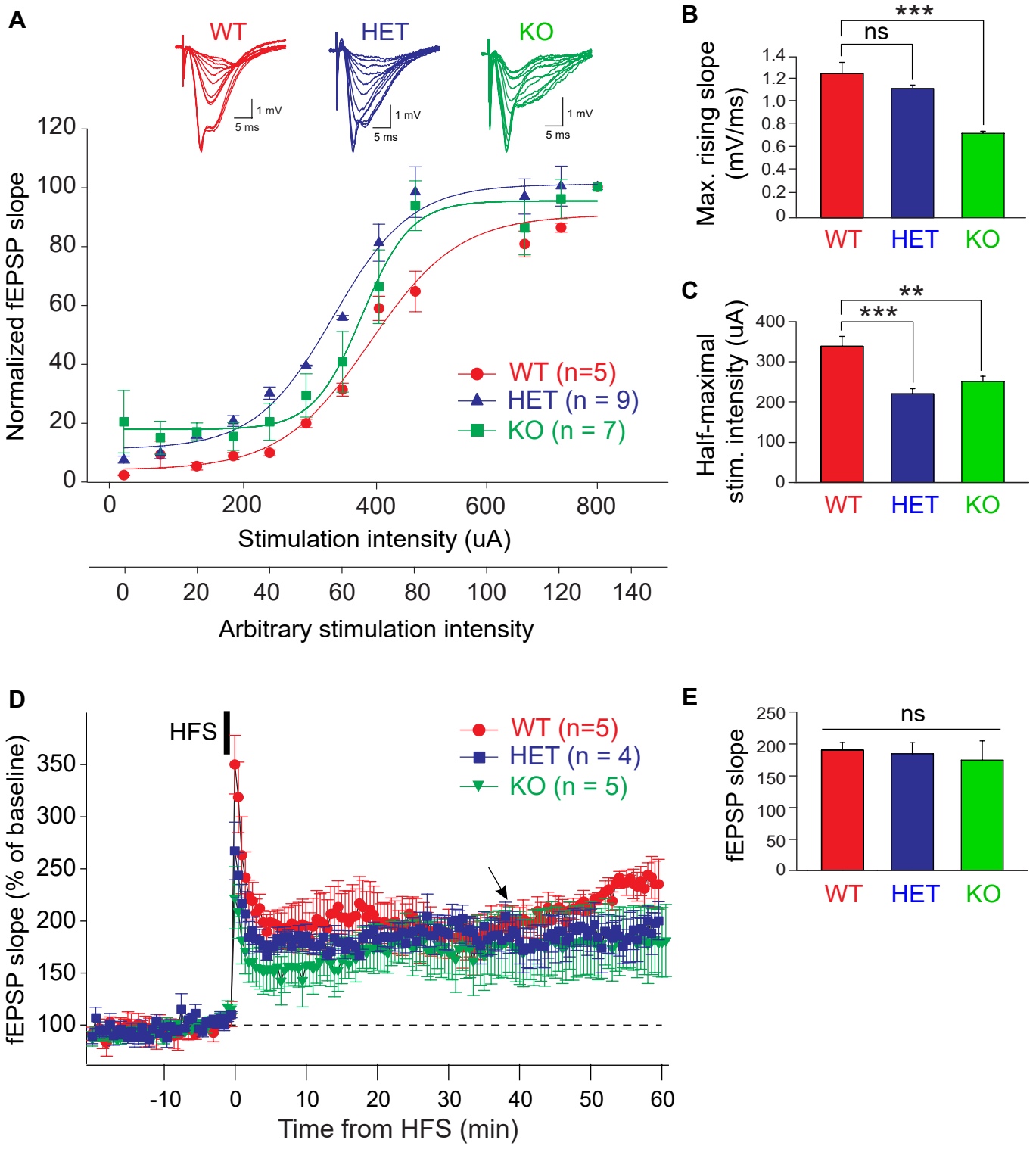
A
WT
HET
KO
1 mV
5 ms
Normalized fEPSP slope
Stimulation intensity (uA)
Arbitrary stimulation intensity
WT (n=5)
HET (n = 9)
KO (n = 7)
B
Max. rising slope (mV/ms)
ns
***
C
Half-maximal stim. intensity (uA)
**
***
D
HFS
fEPSP slope (% of baseline)
Time from HFS (min)
WT (n=5)
HET (n = 4)
KO (n = 5)
E
fEPSP slope
ns

Fig. S2 (*Related to Fig. 3*)**. Electrophysiological analyses in importin α5 knockout hippocampus. A-C**, Input-output relationship between the stimulation magnitude and synaptic response enhancement during basal synaptic activity. **A**, top: representative raw data traces obtained from WT, HET and importin α5 KO mice respectively. Bottom: relationship between the intensity of the presynaptic current and the slope of fEPSP response normalized to the absolute maximal fEPSP slope in each group shown in (**B**) as the maximum change in potential: $[(\mathrm{dV/dt})\mathrm{Max} \equiv \mathrm{dVmax/dt}]$. The absolute maximal fEPSP slope is significantly reduced in importin α5 KOs. **C**, The half-maximal stimulation intensity is reduced both in HET and KO. The half-maximal stimulation intensity was derived from sigmoidal fit equation $\left(\mathrm{W} = \mathrm{Wmax}/\left(1 - \mathrm{e}^{(-\mathrm{I}1/2)}/\mathrm{a}\right)\right) + \mathrm{const.}$, where $\mathrm{W} = \mathrm{dV/dt}$, $\mathrm{Wmax} = \mathrm{dVmax/dt}$, $\mathrm{I}\,1/2$ is the half-maximal stimulation intensity and a is the sigmoidal function slope. **D, E**, LTP experiment. **D**, Summary of 1 hr LTP recordings from hippocampal slices of WT, HET, and KO mice. The LTP was estimated as a stable increase in fEPSP slope after high frequency stimulation (HFS) composed of two 1 s-long trains of 100 Hz given at time point 0 (HFS and black bold arrow). **E**, Representative normalized fEPSP magnitudes sampled at 42 min after HFS application (black diagonal arrow pointing to the time point). n=5 (WT), 9 (HET), and 7 (α5 KO). ** $p < 0.01$, *** $p < 0.001$ (One way ANOVA with Holm-Sidak post-hoc analysis).

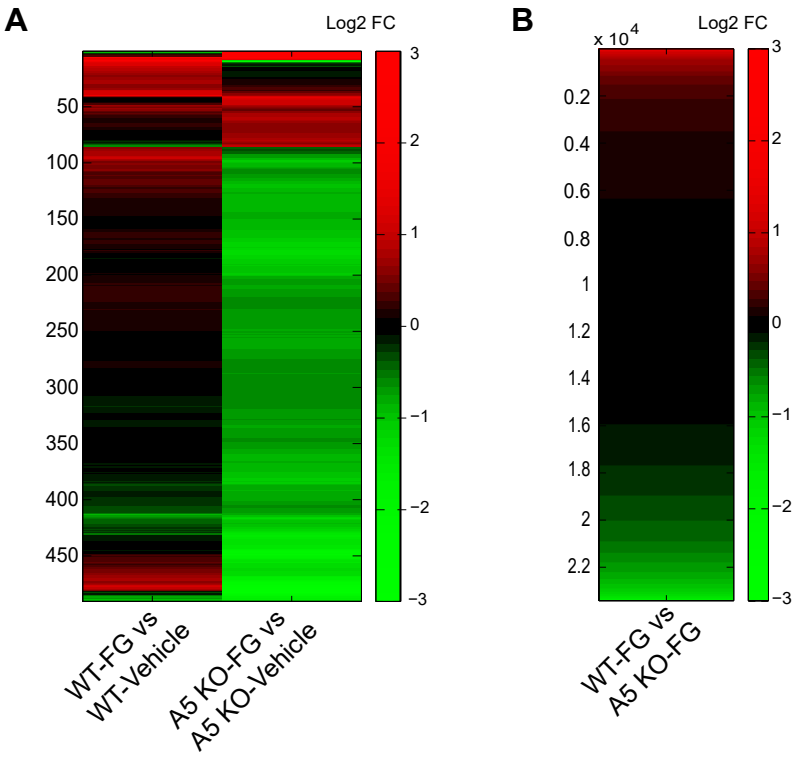

C **Top Networks (Ingenuity)**

1. Organismal Development, Connective Tissue Development and Function, Skeletal and Muscular System
2. Development and Function / Connective Tissue Disorders, Developmental Disorder, Hereditary Disorder
3. Cancer, Organismal Injury and Abnormalities, Reproductive System Disease
4. Molecular Transport, Lipid Metabolism, Small Molecule Biochemistry
5. Inflammatory Disease, Ophthalmic Disease, Organismal Injury and Abnormalities

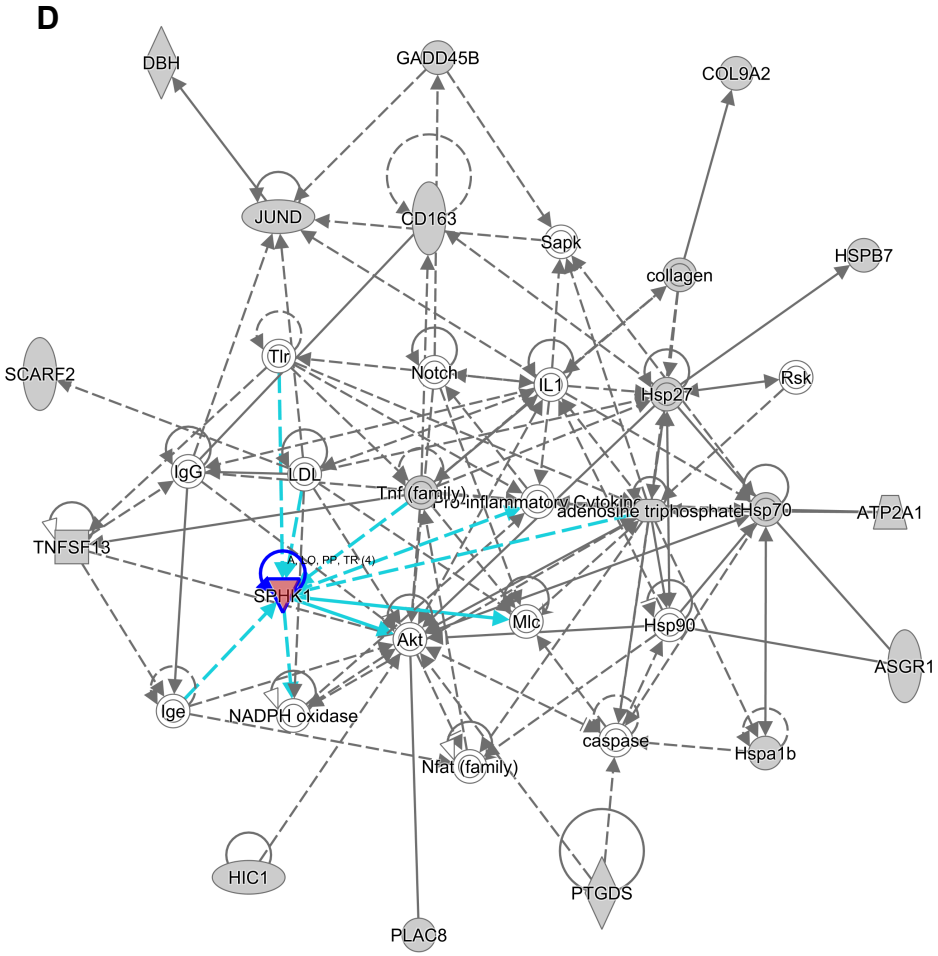

Fig. S3 (*Related to Fig. 5*)**. RNA-seq and network analyses. A**, Heat maps showing log2-normalized fold-change of gene expression in WT+FG vs WT vehicle, α5+FG vs α5-vehicle and **B**, the comparison of WT-FG with α5-FG revealing a larger cohort of almost 600 transcripts that were differentially regulated by FG7142 treatment in knockout versus wild type mice (n = 3 mice per group). See also Table S2. **C**, Identification of signaling networks using the Ingenuity Pathway Analysis program and the candidate genes from the top ranked pathway. **D**, the lipid metabolism network identified as one of the top five signaling networks by Ingenuity contains the Sphk1 gene (red triangle) upregulated in α5 hippocampi.

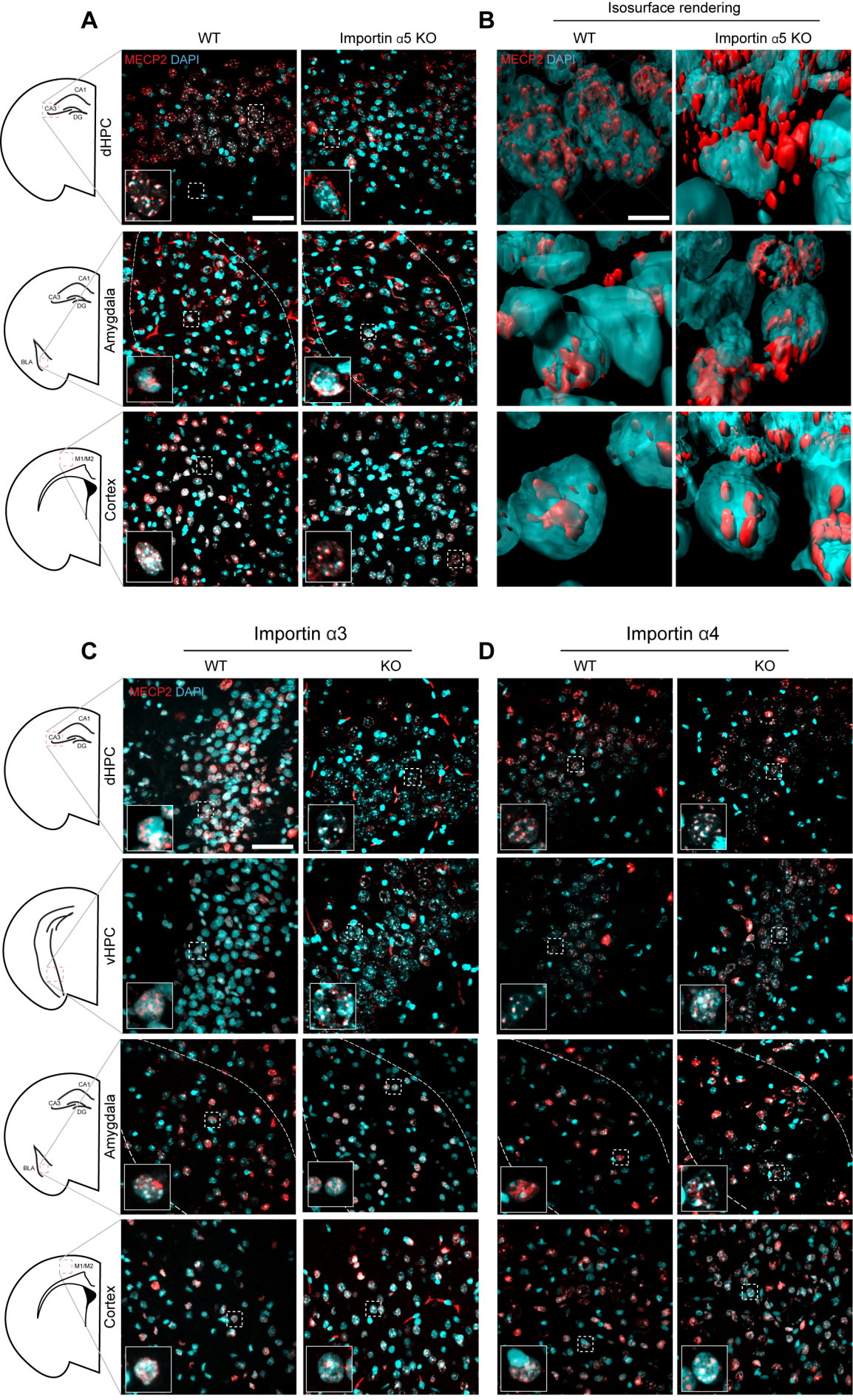
A
WT
Importin α5 KO
MECP2 DAPI
dHPC
Amygdala
Cortex
CA1
CA3
DG
BLA
M1/M2
B
Isosurface rendering
WT
Importin α5 KO
MECP2 DAPI
C
Importin α3
WT
KO
MECP2 DAPI
dHPC
vHPC
Amygdala
Cortex
D
Importin α4
WT
KO
E
WT
α3 KO
Mecp2-DAPI coloc.
(Mander's coefficient m1)
1.0
0.8
0.6
0.4
0.2
0.0
ns
Cortex
dHPC
vHPC
Amyg.
F
WT
α4 KO
Mecp2-DAPI coloc.
(Mander's coefficient m1)
ns
Cortex
dHPC
vHPC
Amyg.

Fig. S4 (*Related to Fig. 5*)**. MeCP2-DAPI colocalization analyses in importin α-deleted brain regions. A,** Immunofluoresence for MECP2 (red) and DAPI nuclear staining (blue) revealing a punctate heterochromatic pattern in neuronal nuclei in the dorsal hippocampus (dHPC; CA3 region), the amygdala and the motor cortex of WT mice, with reduced colocalization in importin α5 knockout dorsal hippocampus while no significant differences were observed in the amygdala and the cortex. **B**, Isosurface rendering of the neuronal nuclei in the respective brain regions (scale bar 50 μm in A and 10 μm in B). **C, D,** Immunofluoresence for MECP2 and DAPI in WT and importin α3 (**C**) and importin α4 (**D**) knockout brain areas and the respective colocalization analyses showing no difference in the subcellular localization of MeCP2 in importin in α3 (**E**) and α4 (**F**) brains (Mander's coefficient m1, $n \geq 3$ for per genotype and per structure). All data error bars represent mean +/- SEM.

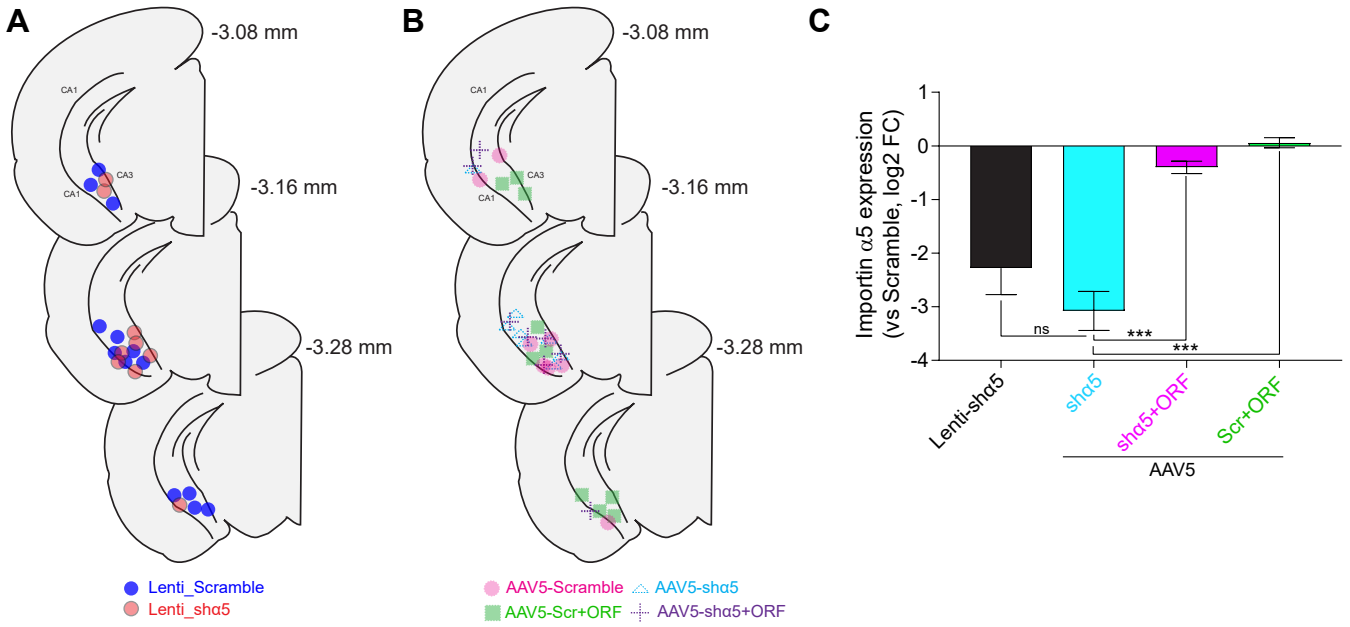
A
-3.08 mm
-3.16 mm
-3.28 mm
CA1
CA3
Lenti_Scramble
Lenti_shα5
B
-3.08 mm
-3.16 mm
-3.28 mm
AAV5-Scramble
AAV5-shα5
AAV5-Scr+ORF
AAV5-shα5+ORF
C
Importin α5 expression (vs Scramble, log2 FC)
ns
***
***
Lenti-shα5
shα5
shα5+ORF
Scr+ORF
AAV5

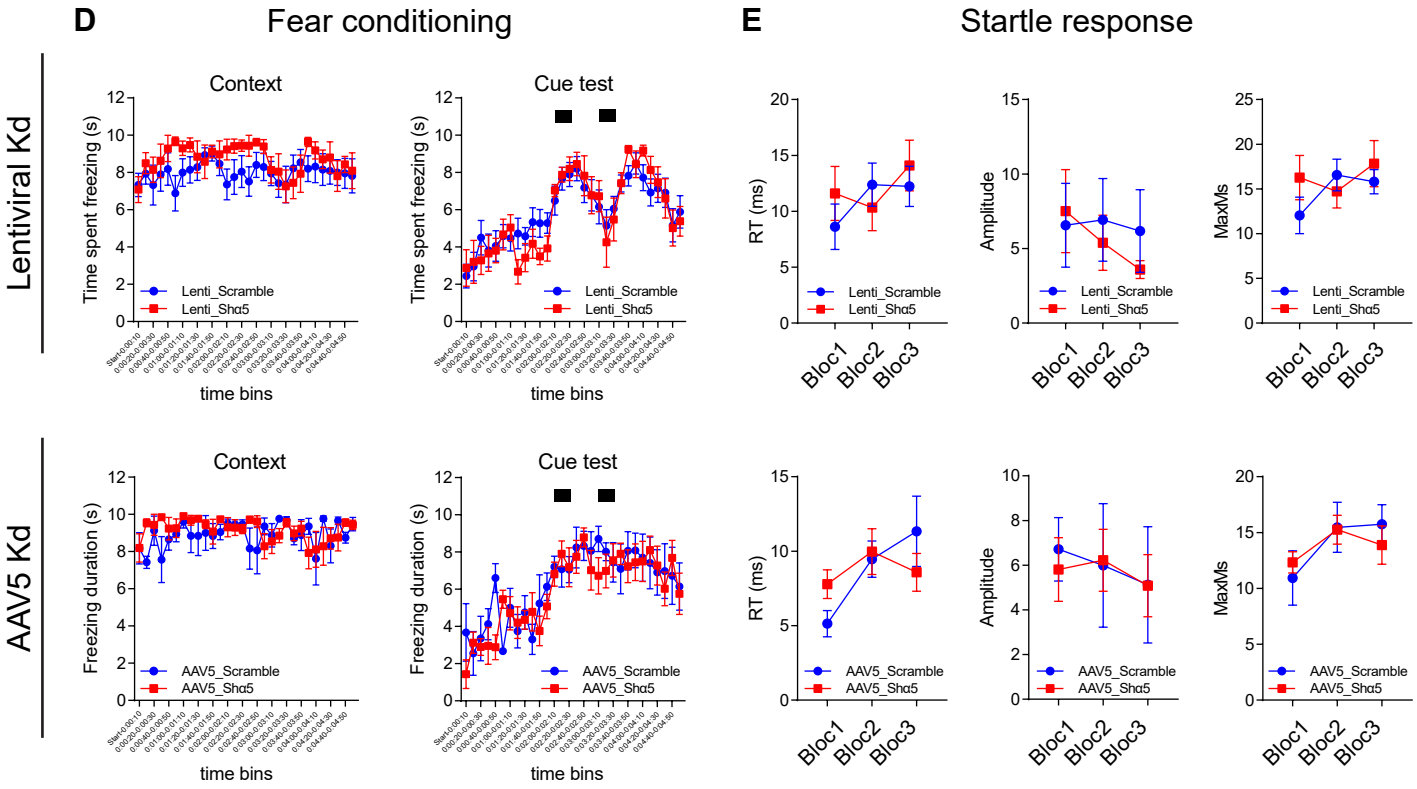
D
Fear conditioning
E
Startle response
Lentiviral Kd
AAV5 Kd
Context
Cue test
Time spent freezing (s)
Freezing duration (s)
time bins
Lenti_Scramble
Lenti_Shα5
AAV5_Scramble
AAV5_Shα5
RT (ms)
Amplitude
MaxMs
Bloc1
Bloc2
Bloc3

Fig. S5 (*Related to Fig. 6*)**. Acute knockdown of importin α5. A, B,** Schematic representation of the virus injection position in the ventral hippocampus. The brain plates illustrating the injection sites were designed in accordance to the Paxinos and Franklin Mouse Brain Atlas (distance from Bregma are shown in mm). **C,** RT-qPCR results showing the knockdown of importin α5 in the vHPC 5 weeks after injection (after completion of behavioral study) of the respective virus preparations. Results expressed as log2 fold-change vs. the respective scramble-injected control condition. *** $p < 0.001$ (Unpaired two-tailed *t*-test). Panels **D, E** respectively show the absence of differences in the fear conditioning freezing behavior and startle response of Lentivirus and AAV5-injected mice. All data error bars represent mean +/- SEM.

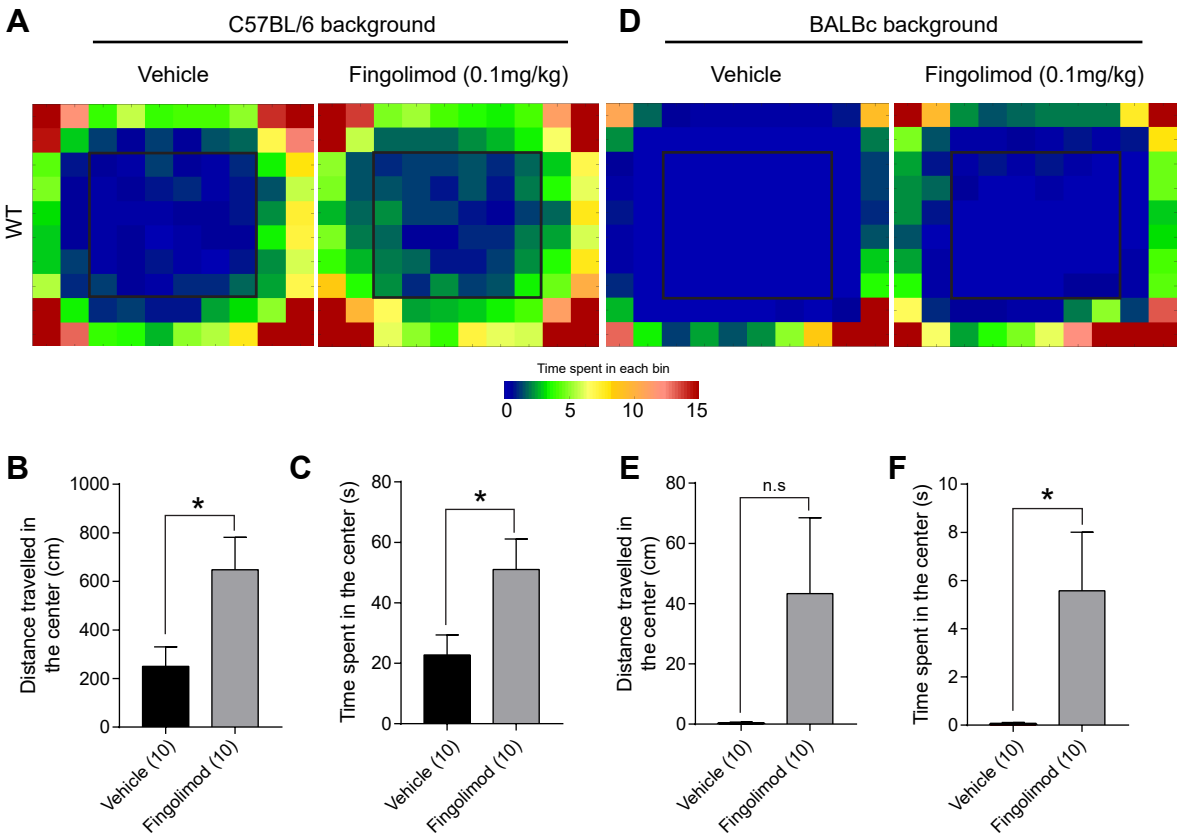
A
C57BL/6 background
Vehicle
Fingolimod (0.1mg/kg)
WT
D
BALBc background
Vehicle
Fingolimod (0.1mg/kg)
Time spent in each bin
0
5
10
15

B
Distance travelled in the center (cm)
1000
800
600
400
200
0
*
Vehicle (10)
Fingolimod (10)
C
Time spent in the center (s)
80
60
40
20
0
*
Vehicle (10)
Fingolimod (10)
E
Distance travelled in the center (cm)
80
60
40
20
0
n.s
Vehicle (10)
Fingolimod (10)
F
Time spent in the center (s)
10
8
6
4
2
0
*
Vehicle (10)
Fingolimod (10)

Fig. S6 (*Related to Fig. 7*)**. Effects of fingolimod in open field tests. A, D**, Density map of mouse exploratory activity in the EPM test showing the effects of fingolimod on wild type C57BL/6 (A) and BALB/c mice (D). **B, C**, Fingolimod has clear and robust anxiolytic effects on C57BL/6 mice, increasing the distance travelled and the time spent in the center of the OF arena. **E, F**, The same experiment in BALB/c mice likewise reveals anxiolytic effects of fingolimod, number of animals per group indicated in parentheses, * $p < 0.05$ (two-tailed t-test (B, C, E, F). All data error bars represent mean +/- SEM.